Molecular Biology of the Cell
Vol. 9, 469–481, February 1998

Identification of a Human VPF/VEGF 3′ Untranslated Region Mediating Hypoxia-induced mRNA Stability

Kevin P. Claffey,*† Shu-Ching Shih,* Andrew Mullen,* Suzan Dziennis,* Jennifer L. Cusick,* Kristin R. Abrams,* Sam W. Lee,‡ and Michael Detmar*§

Departments of *Pathology, ‡Medicine, and §Dermatology, Beth Israel Deaconess Medical Center and Harvard Medical School, Boston, Massachusetts 02215

Submitted September 4, 1997; Accepted November 7, 1997
Monitoring Editor: Joan Massague

Hypoxia is a prominent feature of malignant tumors that are characterized by angiogenesis and vascular hyperpermeability. Vascular permeability factor/vascular endothelial growth factor (VPF/VEGF) has been shown to be up-regulated in the vicinity of necrotic tumor areas, and hypoxia potently induces VPF/VEGF expression in several tumor cell lines in vitro. Here we report that hypoxia-induced VPF/VEGF expression is mediated by increased transcription and mRNA stability in human M21 melanoma cells. RNA-binding/electrophoretic mobility shift assays identified a single 125-bp AU-rich element in the 3′ untranslated region that formed hypoxia-inducible RNA-protein complexes. Hypoxia-induced expression of chimeric luciferase reporter constructs containing this 125-bp AU-rich hypoxia stability region were significantly higher than constructs containing an adjacent 3′ untranslated region element without RNA-binding activity. Using UV-cross-linking studies, we have identified a series of hypoxia-induced proteins of 90/88 kDa, 72 kDa, 60 kDa, 56 kDa, and 46 kDa that bound to the hypoxia stability region element. The 90/88-kDa and 60-kDa species were specifically competed by excess hypoxia stability region RNA. Thus, increased VPF/VEGF mRNA stability induced by hypoxia is mediated, at least in part, by specific interactions between a defined mRNA stability sequence in the 3′ untranslated region and distinct mRNA-binding proteins in human tumor cells.

INTRODUCTION

Vascular permeability factor/vascular endothelial growth factor (VPF/VEGF)[1] is a potent activator of microvascular permeability in vivo and an endothelial cell-specific mitogen in vitro (Connolly *et al.*, 1989; Ferrara and Henzel, 1989; Gospodarowicz *et al.*, 1989; Keck *et al.*, 1989; Leung *et al.*, 1989; Levy *et al.*, 1989; Conn *et al.*, 1990; Senger *et al.*, 1990; Ferrara *et al.*, 1991a,b; Dvorak *et al.*, 1992). VPF/VEGF expression has been closely associated with the pathological angiogenesis observed in malignant tumors (Plate *et al.*, 1992; Brown *et al.*, 1993a,b; Weindel *et al.*, 1994; Brown *et al.*, 1995a,b), diabetic retinopathy (Adamis *et al.*, 1994; Aiello *et al.*, 1994), retinopathy of prematurity (Alon *et al.*, 1995; Pierce *et al.*, 1995; Stone *et al.*, 1995), rheumatoid arthritis (Fava *et al.*, 1994), and coronary artery disease (Sabri *et al.*, 1991; Ladoux and Frelin, 1993; Hashimoto *et al.*, 1994). Tissue hypoxia is a common feature in many of these diseases and VPF/VEGF expression is dramatically up-regulated in human solid tumors adjacent to sites of focal necrosis (Plate *et al.*, 1992; Shweiki *et al.*, 1992; Brown *et al.*, 1993).

Hypoxia-stimulated VPF/VEGF expression has been attributed to increases in both transcriptional and posttranscriptional mechanisms (Ikeda *et al.*, 1995; Stein *et al.*, 1995; Levy *et al.*, 1996a,b). The transcriptional up-regulation of VPF/VEGF under hypoxia appears to be a common mechanism in a multitude of

† Corresponding author.

[1] Abbreviations used: ARE, adenylate–uridylate-rich region; EMSA, electrophoretic mobility shift assay; GM-CSF, granulocyte macrophage-colony stimulating factor; HSR, hypoxia stability element; UTR, untranslated region; VEGF, vascular endothelial growth factor; VPF, vascular permeability factor.

tumor cell types and has been linked to 5′ flanking elements of the *VPF/VEGF* gene that contain binding sites for the hypoxia-regulated transcription factor, hypoxia-inducible factor 1 (Wang and Semenza, 1993; Minchenko *et al.*, 1994; Levy *et al.*, 1995; Liu *et al.*, 1995). Hypoxia has also been shown to increase VPF/VEGF mRNA stability in several rodent and human cell lines (Ikeda *et al.*, 1995; Mukhopadhyay *et al.*, 1995; Shima *et al.*, 1995; Stein *et al.*, 1995; Levy *et al.*, 1996a,b). VPF/VEGF belongs to a group of genes with labile mRNAs, including c-*fos*, c-*myc*, and granulocyte-macrophage colony-stimulating factor (GM-CSF) (Schuler and Cole, 1988; Brewer, 1991; Vakalopoulou *et al.*, 1991; You *et al.*, 1992; Chen and Shyu, 1995). Many of these mRNAs possess adenylate–uridylate-rich elements (AREs) in their 3′ untranslated regions (3′ UTR), which are thought to regulate mRNA stability (Chen and Shyu, 1995). These labile mRNAs have been shown to be transiently stabilized by various stimuli including phorbol ester, calcium ionophore, cyclic adenosine monophosphate, and tumor necrosis factor-α (Malter and Hong, 1991; Stephens and Bauerle, 1992).

Recently, a family of proteins has been described that bind to the consensus AUUUA sequence, which is frequently present in the AREs of labile mRNAs. These proteins, which range from 15 to 40 kDa, include AU-binding factor 1 (Brewer, 1991; Zhang *et al.*, 1993), AU-A/Band/C (Bohjanen *et al.*, 1991, 1992; Katz *et al.*, 1994), AU-binding factor (Gillis and Malter, 1991; Malter and Hong, 1991), AU-binding protein (Nagy and Rigby, 1995), AUH and enoyl CoA-hydratase isoform (Nakagawa *et al.*, 1995), interleukin 1 mRNA-binding protein (Gorospe and Baglioni, 1994), GM-CSF/c-*myc*/c-*fos* mRNA-binding protein (Shaw and Kamen, 1986; Malter, 1989; Vakalopoulou *et al.*, 1991; You *et al.*, 1992), and surprisingly, glyceraldehyde-3-phosphate dehydrogenase (Nagy and Rigby, 1995). This plethora of binding proteins may play a critical role in modulating the rate of degradation of distinct mRNAs that contain AREs.

Recently, it has been reported that the half-life of rat VPF/VEGF mRNA was regulated by both stabilizing and destabilizing AREs in the 3′ UTR (Levy *et al.*, 1996). In addition, hypoxia-inducible proteins of apparent molecular weights of 17,000, 28,000, and 32,000 have been identified that bind to the 3′ UTR (Levy *et al.*, 1996).

Because hypoxia-induced VPF/VEGF expression plays an important role in promoting tumor angiogenesis and progression of several human malignant tumors, we sought to characterize the mechanisms that mediate hypoxia-induced VPF/VEGF expression in human tumor cells. In particular, the contribution of VPF/VEGF mRNA stability and its role in promoting hypoxia-induced VPF/VEGF expression was examined. Here we report the identification of elements in the 3′ UTR of the human VPF/VEGF mRNA that bind to hypoxia-induced proteins, the role of these elements in hypoxia-mediated mRNA accumulation, and the partial characterization of the RNA-binding proteins involved.

MATERIALS AND METHODS

Cell Lines, Culture Conditions, and Transfection Procedures

The human melanoma cell line M21 was obtained from Dr. Romaine Saxton (University of California, Los Angeles, CA). Cells were cultured in DMEM supplemented with 10% fetal bovine serum, 2 mM L-glutamine, 10 U/ml penicillin, and 10 μg/ml streptomycin. Normoxic cell cultures were maintained in a humidified Queue (Asheville, NC) incubator in an atmosphere of 5% CO_2, 21% O_2, and 74% N_2 at 37°C. Hypoxia experiments were performed for the indicated times in a humidified triple gas Heraeus model 6060 incubator (Hanau, Germany) calibrated to deliver 5% CO_2, 2% O_2, and 93% N_2 at 37°C. Cells were transfected with the calcium phosphate method as described previously (Claffey *et al.*, 1996). Cell extracts were made with passive lysis buffer and luciferase assays were performed with a Luciferase Assay kit (Promega, Madison, WI). Total-cell RNA was isolated and analyzed for VPF/VEGF mRNA expression by Northern blot analysis as outlined below. VPF/VEGF secretion was analyzed by a human VPF/VEGF enzyme-linked immunosorbent assay (R&D Systems, Minneapolis, MN).

RNA Isolation and Northern Blot Analysis

Total cellular RNA was isolated from cultured cell lines using Trizol reagent (Life Technologies, Gaithersburg, MD) according to the manufacturer's instructions. Northern blot analyses were performed as described previously (Claffey *et al.*, 1996). $VPF/VEGF_{165}$ hybridization probe was an *Acc*I–*Nco*I fragment (823 bp) encompassing the coding region and 330 bp of 3′ UTR of the FL cDNA clone (see below). A ribosome-associated protein cDNA, 36B4, was used as a control (Masiakowski *et al.*, 1983). Probes were prepared by the [α-^{32}P]dCTP random-primed synthesis method using the Multiprime kit (Amersham, Arlington Heights, IL). Blots were washed at high stringency (1% SDS, 0.1× SSC at 60°C), exposed to x-ray film (Kodak X-Omat AR, Eastman Kodak, Rochester, NY) for up to 24 h, and subjected to phosphorimage quantification (Molecular Dynamics, Sunnyvale, CA).

Cloning, Sequencing, Subcloning, and Analysis of Human $VPF/VEGF_{165}$ cDNA

A partial human VPF/VEGF cDNA clone was isolated by reverse transcription-polymerase chain reaction (PCR) amplification using human VPF/VEGF sequence-specific primers. The partial PCR product of approximately 300 bp was sequenced and used as a probe to obtain the FL clones by screening a cDNA library prepared from normal human mammary epithelial cells (76N λ ZAP library, Stratagene, La Jolla, CA) (Lee *et al.*, 1991). Approximately 10^5 recombinant phages ($2–4 \times 10^3$ per 150-mm dish) were transferred in duplicate to nitrocellulose filters and hybridized overnight at high-stringency conditions. The longest cDNA clones obtained by library screening were excised and ligated into pBluescript vectors (Stratagene) and were further characterized and sequenced by the dideoxy chain termination sequencing method (Sequenase kit version 2.0, United States Biochemical, Cleveland, OH). A 3.6-kb complete cDNA encoding the $VPF/VEGF_{165}$ amino acid isoform was isolated and sequenced and contained 701 bp of 5′ UTR and 1.9 kb of 3′ UTR (GenBank access no. AF022375). The coding sequence was in complete agreement with the $VPF/VEGF_{165}$ sequence described

previously (Tischer *et al.*, 1991). A subclone of the FL cDNA was made that deleted the entire 5′ UTR and coding region and maintained untranslated sequences from 219 bp to 1890 bp downstream of the stop codon. Oligonucleotide primer pairs used for PCR amplification of 3′ UTR sequences were: 3′ hypoxia stability region (3′ HSR) sense 5′-TAGACACACCCACCCACATA-3′ and antisense 5′-AACATTAGCACTGTTAATT-3′; 3′ control region 1 (3′ CR-1) sense 5′-GATGTATGTGACTGCTGTGG-3′ and antisense 5′-CATGCCCTGGCCTTGCACATTC-3′; and 3′ control region 2 (3′ CR-2) sense 5′-GTGCAAGGCCAGGGCATGGG-3′ and antisense 5′-GTCCTGAAGCTCCCCAAACTCC-3′. Amplified PCR products were ligated into pCR-Script vector (Stratagene) according to the manufacturer's instructions and sequenced to confirm identity to the original.

Transcription Run-Off Assays

M21 and U373 cells were incubated for 24 h under normoxic or hypoxic conditions. Five × 100-mm dishes (approximately 1×10^7 cells) were washed twice with ice-cold phosphate-buffered saline, lysed by adding 0.5 ml per dish of lysis buffer (10 mM Tris-HCl, pH 7.4, 10 mM NaCl, 3 mM $MgCl_2$, 0.35% sucrose, and 0.5% Nonidet P-40), and scraped into microfuge tubes and placed on ice for 5 min. Nuclei were pelleted for 3 min at 500 × *g*. The supernatant was removed and the pellets were carefully resuspended in 0.5 ml of lysis buffer and recentrifuged for 3 min at 500 × *g*. Nuclei were suspended in 50 μl of glycerol storage buffer (50 mM Tris-HCl, pH 8.3, 5 mM $MgCl_2$, 300 mM KCl, 10 mM EDTA, and 40% glycerol), snap frozen in liquid nitrogen, and stored at −80°C. For run-off transcription reactions, frozen nuclei were thawed on ice and centrifuged at 100 × *g* for 2 min. Pelleted nuclei were resuspended in 50 μl of reaction buffer [5 mM Tris-HCl, pH 8.0, 2.5 mM $MgCl_2$, 150 mM KCl, 0.5 mM rNTP [A,G,C], 0.7 μM rUTP, 2.5 mM dithiothreitol, and 5 U RNAsin (Promega)]. After addition of 100 μCi [α-^{32}P]UTP (>3000 Ci/mmol), the suspended nuclei were incubated at 30°C for 23 min and mixed every 5 min to prevent clumping. Transcription was terminated and total RNA was isolated by the addition of 40 μg of glycogen carrier and 0.8 ml of Trizol reagent. Chloroform was added and phases were separated by centrifugation at 14,000 × *g* for 10 min at 4°C. Supernatants were extracted with phenol/chloroform, precipitated with 0.5 volume of isopropanol, and RNA/glycogen pellets were washed with 100% ice-cold ethanol. The radiolabeled RNA pellets were resuspended in 0.05 ml of diethyl pyrocarbonate-treated water containing 10 mM β-mercaptoethanol, and an aliquot was counted by liquid scintillation counting.

Slot blots used for RNA hybridizations were made with 5 μg of hVPF/VEGF, hGlut-1, 36B4, and 2.5 μg of glyceraldehyde-3-phosphate dehydrogenase (GAPDH) cDNAs denatured with 100 mM NaOH at 100°C for 10 min, neutralized with NH_4OAc to 1 M final concentration, and directly blotted onto Biotrans (New England Nuclear, Boston, MA) nylon membranes (ICN, Costa Mesa, CA) using a vacuum slot blot apparatus (Schleicher & Schuell, Keene, NH). Membranes were subsequently washed twice with 2× SSC and baked at 80°C for 1 h. Blots were prehybridized for 6 h at 65°C in hybridization buffer (50 mM peperazine-*n*, *N*′-bis(2-ethanesulfonic acid), pH 6.5, 50 mM sodium phosphate mono/dibasic, pH 7.0, 20 mM NaCl, 5% SDS, 2.5 mM EDTA, and 50 μg/ml of denatured salmon sperm DNA). Hybridizations were performed with equal amounts of labeled nuclear RNA at 1×10^6 dpm/ml of hybridization buffer for 20 h at 65°C. Blots were then washed twice at room temperature for 20 min and once at 55°C for 20 min in 1.0% SDS-1× SSC. Blots were exposed for 2 d to x-ray film (Kodak X-Omat AR) and subjected to phosphorimage analysis (Molecular Dynamics).

Determination of VPF/VEGF mRNA Half-Life in Cultured Cells

Cells were grown under normoxic or hypoxic conditions in complete media containing 10% fetal bovine serum for 20 h before the addition of actinomycin D at 5 μg/ml. Cells were returned to normoxic or hypoxic incubators for the indicated time before rapid RNA isolation. Total RNA (10 μg) was analyzed by Northern blot as outlined above, and only the mature VPF/VEGF mRNA signal (4.2 kb) was quantified by phosphorimage analysis. The VPF/VEGF mRNA signal was normalized to the 28S ribosomal signal. Least squares regression analysis of the resulting line was performed (Kaleidagraph, Synergy Software, Reading, PA), and half-life values were determined from the regression curves.

RNA-binding/Electrophoretic Mobility Shift Assay (EMSA)

Cells were grown under normoxic or hypoxic conditions, and cytoplasmic extracts were prepared at 4°C with slight modifications of the method described previously (Wang *et al.*, 1995). Briefly, cells were washed three times in ice-cold phosphate-buffered saline and then lysed with 0.5 ml per 100-mm dish of lysis buffer [50 mM HEPES, pH 7.5, 10 mM sodium pyrophosphate, 150 mM NaCl, 100 mM NaF, 0.2 mM $NaOVa_4$, 1 mM EGTA, 1.5 mM $MgCl_2$, 1% Triton X-100, 10% glycerol, 5 mM 4-(2-aminoethyl)benzene-sulfonyl fluoride, and 3 μg/ml of aprotinin, leupeptin, and soybean trypsin inhibitor]. Cells were collected with a cell lifter, mixed well by pipetting, and placed into microcentrifuge tubes. The tubes were incubated on ice for 10 min, centrifuged at 14,000 × *g* for 10 min, and supernatants were frozen in liquid nitrogen and stored at −80°C. Protein concentrations were determined using the Bio-Rad DC reagent assay (Bio-Rad, Hercules, CA).

RNA transcripts were synthesized from linearized DNA templates using either T3 or T7 bacteriophage RNA polymerases with the RNA Transcription kit (Stratagene) according to the manufacturer's instructions. Transcription reactions were treated with RNase-free DNase (Promega) for 15 min at 37°C, were extracted once with phenol/chloroform, and free ribonucleotides were removed using RNase-free G-50 spin columns (Boehringer Mannheim, Indianapolis, IN). Radiolabeled RNAs were analyzed for complete transcription by denaturing sequencing gels and were quantitated by liquid scintillation counting. Nonradioactive RNAs were evaluated by agarose gel electrophoresis and ethidium bromide staining to quantify relative amounts using RNA markers (Life Technologies) as standards.

Radiolabeled RNA transcripts (200,000 cpm/reaction) were combined with protein extract (30 μg) in binding buffer for a final concentration of 10 mM HEPES (pH 7.5), 5 mM $MgCl_2$, 50 mM KCl, 0.5 mM EGTA, 0.5 mM dithiothrietol, 10% glycerol, 100 μg/ml tRNA, and 5 mg/ml heparin. The reaction mixture was incubated at 30°C for 20 min. Ribonuclease T1 (40 units) (Boehringer Mannheim) alone or in combination with 1 μg of ribonuclease A (Boehringer Mannheim) was added and incubated for 15 min at room temperature. The reaction mixtures were electrophoresed for 2 h in a 4% native polyacrylamide gel in 0.5× Tris borate EDTA buffer. Gels were dried and exposed to x-ray film, and RNA complexes were quantified by phosphorimage analysis.

UV-cross-linking studies were performed by UV-cross-linking RNA-binding reactions in a Stratalinker (Stratagene) for 10 min (total energy = 1800 J/cm^2). Ribonuclease T1 (40 units) and A (1 μg) were then added and incubated at room temperature for 15 min before the addition of SDS sample buffer containing reducing agent (10 mM Tris-HCl, pH 6.8, 100 mM dithiothrietol, 0.15% SDS, 10% glycerol, and 0.05% bromophenol blue). The samples were boiled for 5 min before electrophoresis on a 10% acrylamide SDS-polyacrylamide gel.

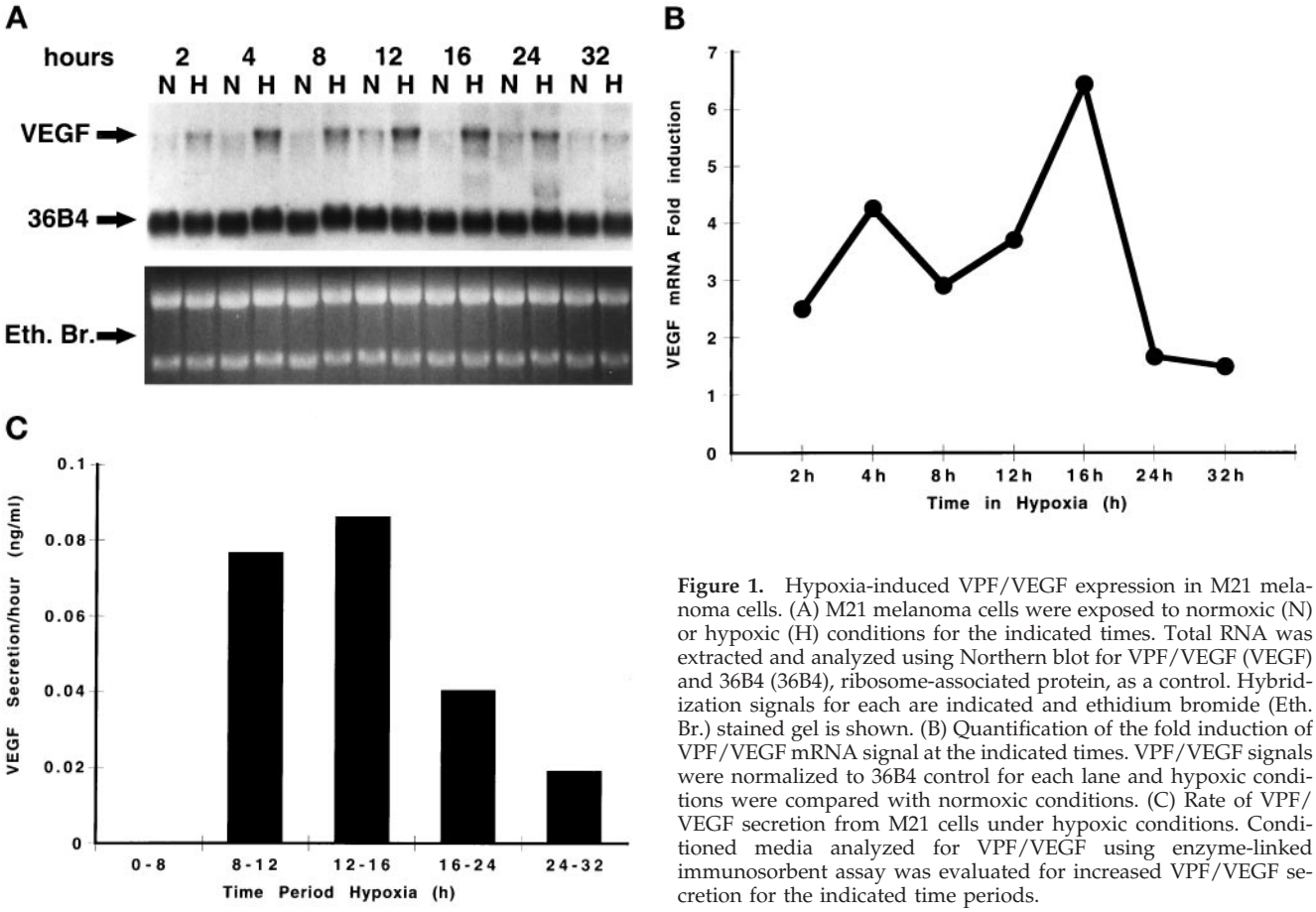

Figure 1. Hypoxia-induced VPF/VEGF expression in M21 melanoma cells. (A) M21 melanoma cells were exposed to normoxic (N) or hypoxic (H) conditions for the indicated times. Total RNA was extracted and analyzed using Northern blot for VPF/VEGF (VEGF) and 36B4 (36B4), ribosome-associated protein, as a control. Hybridization signals for each are indicated and ethidium bromide (Eth. Br.) stained gel is shown. (B) Quantification of the fold induction of VPF/VEGF mRNA signal at the indicated times. VPF/VEGF signals were normalized to 36B4 control for each lane and hypoxic conditions were compared with normoxic conditions. (C) Rate of VPF/VEGF secretion from M21 cells under hypoxic conditions. Conditioned media analyzed for VPF/VEGF using enzyme-linked immunosorbent assay was evaluated for increased VPF/VEGF secretion for the indicated time periods.

RESULTS

Hypoxia-induced VPF/VEGF mRNA Expression in M21 Melanoma Cells Is Mediated by Increased Transcription and mRNA Stability

A human M21 melanoma tumor cell line was selected for study of the regulation of VPF/VEGF expression by hypoxia. Treatment of M21 cells with hypoxia over a time course of 32 h revealed a maximal VPF/VEGF expression at 12–16 h (Figure 1A). Prolonged hypoxia (>32 h) resulted in cell death as determined by cell detachment from plates. Hypoxia induction of steady-state VPF/VEGF mRNA expression in M21 cells was maximally up-regulated at 16 h by 6.5-fold (Figure 1B). The enhanced mRNA expression resulted in a comparable increase in VPF/VEGF secretion with maximal secretion rates between 8 and 16 h as determined by an enzyme-linked immunosorbent assay (Figure 1C). In contrast, the expression of the ribosome-associated protein mRNA, 36B4, was not affected by hypoxia.

To more clearly define the cellular mechanisms controlling the induction of VPF/VEGF mRNA expression in these tumor cell lines, the regulation of transcription and mRNA stability were investigated separately. To analyze transcriptional control, run-off transcription assays were performed that showed a 2.7-fold up-regulation of VPF/VEGF mRNA transcription by hypoxia in M21 cells compared with the 36B4 control, which was unaffected (Figure 2A). In comparison, GAPDH showed a 3-fold and Glut-1 a 2.5-fold transcription up-regulation, consistent with the increased hypoxic expression of both of these genes (Graven *et al.*, 1994; Ebert *et al.*, 1995). The level of increased gene transcription, however, only partially accounted for the total increase in VPF/VEGF mRNA expression observed by Northern blot analysis, suggesting an additional effect of hypoxia on mRNA stability.

To examine the effect of hypoxia on the stability of VPF/VEGF mRNA, M21 cells were treated with the transcriptional inhibitor actinomycin D in the presence or absence of hypoxia. The rate of decay of the mature VPF/VEGF mRNA (4.2 kb) was determined by Northern blot hybridization over a 3-h treatment period (Figure 2B). In the example shown, hypoxic conditions significantly increased the half-life of VPF/

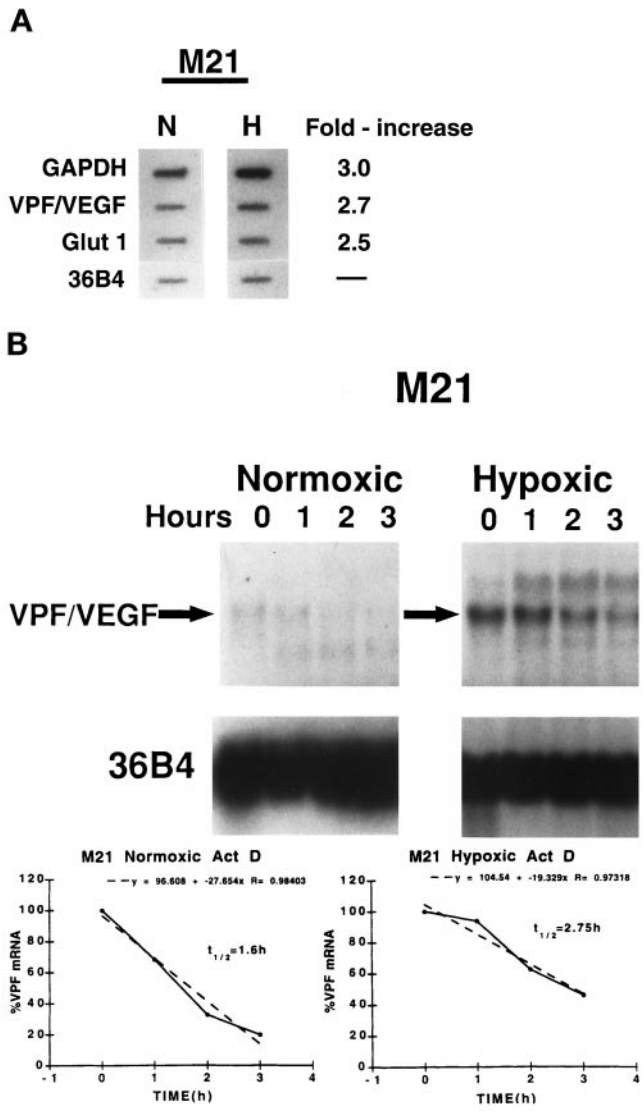

Figure 2. Hypoxia-induced VPF/VEGF transcription and mRNA stability in M21 melanoma cells. (A) Transcription run-off assay of M21 cells exposed to 24 h normoxic (N) or hypoxic (H) conditions. Total radiolabeled RNAs were hybridized to denatured cDNA templates encoding GAPDH, VPF/VEGF, Glut-1, and 36B4. Fold induction by quantification is indicated. (B) Representative Northern blot analysis of M21 cells preincubated for 20 h under normoxic or hypoxic conditions. Actinomycin D was added at time 0 and total RNA was isolated after up to 3 h. Mature VPF/VEGF mRNA signal and 36B4 control are indicated by arrows. VPF/VEGF mRNA decay curves and mRNA half-life ($t_{1/2}$) are presented below each Northern blot.

VEGF mRNA from 1.6 to 2.75 h. A similar experiment performed in triplicate revealed a $t_{1/2}$ for VPF/VEGF mRNA of 1.47 ± 0.15 h for normoxia and 2.62 ± 0.13 h for hypoxia. This induction was statistically significant using Student's t test at $p = 0.0005$, which is considered extremely significant. Thus, a 1.8-fold increase in mRNA stability was observed in the M21 cells along with a 2.75-fold increase in transcription, yielding the approximate 6- to 7-fold increase observed in the steady-state mRNA level. These data indicated that increased mRNA stability significantly contributes to the total hypoxia-induced VPF/VEGF expression in M21 cells.

Cloning and Sequence of a Human VPF/VEGF$_{165}$ FL cDNA Containing the Complete 3′ UTR

Although the transcriptional regulation of the *VPF/VEGF* gene is thought to be mediated through 5′ flanking gene sequences containing binding sites for the transcription factor, hypoxia-inducible factor 1, the mechanisms regulating mRNA stability of human VPF/VEGF have not been characterized in detail. To evaluate VPF/VEGF mRNA sequences for potential interaction with cellular RNA-binding proteins affecting mRNA stability, a human FL VPF/VEGF$_{165}$ cDNA was cloned from a human breast epithelial cell library. The cDNA clone contained 0.7 kb of the estimated 1.1-kb 5′ UTR described previously (Tischer *et al.*, 1991), the coding region of 573 bp, and a 1.9-kb 3′ UTR. The 3′ UTR has been identified in several genes as the location of mRNA stabilizing or destabilizing elements. The sequence of the human VPF/VEGF 3′ UTR and key potential mRNA regulatory sites are shown in Figure 3A. The 3′ UTR sequence extends from one base after the TGA stop codon to 1890 bp and contains two consensus AAUAAA polyadenylation sites within the 3′ UTR at 388 bp and 1626 bp. Two complete consensus sequences for the mRNA destabilizing elements 5′-UUAUUUA(U/A)(U/A)-3′ (Lagnado *et al.*, 1994; Zubiaga *et al.*, 1995) were localized at 1231 bp and 1734 bp in the 3′ UTR. Several studies suggested that multiple copies of the AUUUA base sequence might affect mRNA stability (Chen and Shyu, 1995), and five AUUUA sequences were located within the 3′ UTR. Four AU-rich elements were present in pairs, grouped between 358 and 425 bp (AU 1 and AU 2) and between 1549 and 1598 bp (AU 3 and AU 4). A CU-rich sequence, described as a potential site for binding proteins that bind to the tyrosine hydroxylase mRNA (Czyzyk-Krzeska *et al.*, 1994a,b; Czyzyk-Krzeska and Beresh, 1996) was located between 1343 bp and 1358 bp.

An AU-rich Sequence in the 3′ UTR of the Human VPF/VEGF mRNA Mediates Hypoxia-inducible Protein Binding

To further characterize hypoxia-induced VPF/VEGF mRNA stability in M21 melanoma cells, protein-binding studies with radiolabeled mRNAs transcribed from the VPF/VEGF$_{165}$ cDNA template were performed using RNA binding and EMSAs. RNA transcripts (Figure 3B) that covered the FL VPF/VEGF$_{165}$

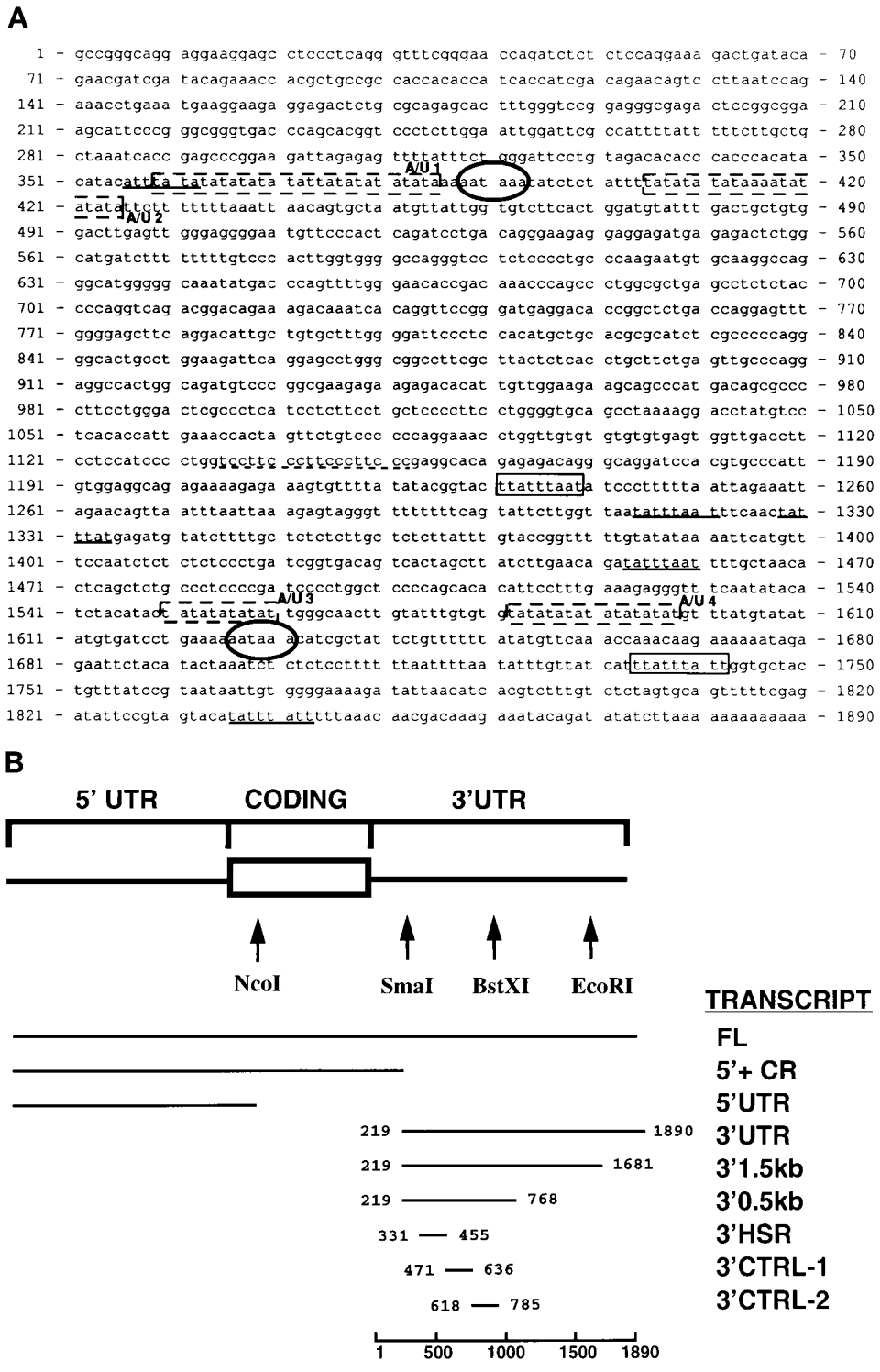

Figure 3. Complete VPF/VEGF$_{165}$ 3′ UTR cDNA sequence and potential regulatory elements. (A) Complete 3′ UTR cDNA sequence beginning with base 1 as the first base after the translation stop codon in the coding region. The polyadenylation site at the 3′ end consists of 13 adenosine residues but is not preceded by a consensus AAUAAA sequence. Two consensus internal polyadenylation sequences are encircled. Two destabilizing elements with the consensus sequence 5′-UUAUUUA(U/A)(U/A)-3′ are indicated (solid boxes). Five underlined sequences show partial consensus sequences that include the AUUUA sequence. Broken boxes indicate AU-rich elements consisting of at least five AU pairs in a row (AU 1–4). The human VPF/VEGF$_{165}$ 3′ UTR sequence is accessible in GenBank accession no. AF022375. (B) Schematic map of VPF/VEGF$_{165}$ FL cDNA and the RNA transcripts used in this study. The numbers indicate base location in the 3′ UTR, and the numerical bar on the bottom represents the 3′ UTR sequence given in A.

mRNA sequence [full length (FL)], the 5′ UTR and [coding region (CR)] (5′ + CR), the 5′ UTR only (5′ UTR), or the 3′ UTR only (3′ UTR) were used as probes for binding studies. As shown in Figure 4A, several RNA–protein complexes were detected when the FL or the 3′ UTR transcripts were used as probes, but not with the 5′ + CR or the 5′ UTR. RNase T1 treatment of the 3′ UTR alone revealed a RNase

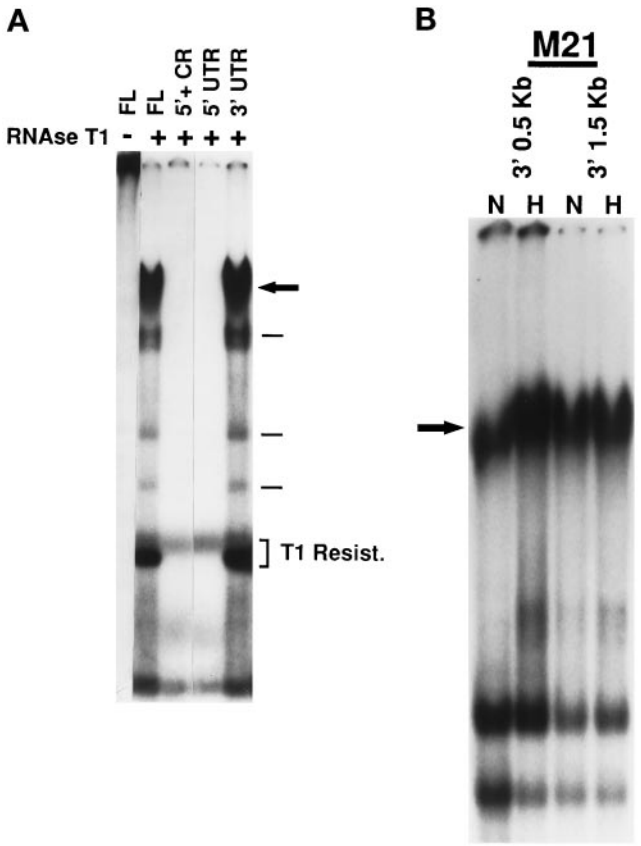

Figure 4. Identification of a 500-bp sequence in the 3′ UTR of VPF/VEGF mRNA that forms hypoxia-inducible RNA–protein complexes. (A) M21 cell extracts were subjected to RNA binding/EMSA with the FL VPF/VEGF, 5′ UTR and coding region (5′+ CR), the 5′ UTR (5′ UTR), and the 3′ UTR (3′ UTR) RNA probes. RNase T1 was not added to a FL probe, indicating minimal endogenous RNase activity (−). RNA–protein complexes are indicated by arrows and lines. RNase T1-resistant bands are indicated (T1 Resist). (B) RNA binding/EMSA of VPF/VEGF subfragment 3′ UTR 1.5-kb probe (3′ 1.5 kb) and the 0.5-kb probe (3′ 0.5 kb). Arrow indicates major complex that is present in normoxic (N) and increased in hypoxic (H) M21 cell extracts.

T1-resistant sequence independent of protein binding. Pretreatment of cell extracts with proteinase or by boiling completely eliminated the binding activity, suggesting that the complexes observed were likely RNA–protein complexes. Antisense transcripts from FL or 3′ UTR sequences did not form RNA–protein complexes, indicating that complex formation was sense-orientation dependent. These data suggested that RNA-binding activity was restricted to the 3′ UTR of the VPF/VEGF mRNA.

When RNA binding/EMSA was performed using two 3′ UTR transcripts of 0.5-kb and 1.5-kb in length (3′ 0.5 kb and 3′ 1.5 kb, see Figure 3B), RNA–protein complexes were readily formed using both the 3′ 1.5-kb and the 3′ 0.5-kb transcripts with normoxic extracts and an increased amount in hypoxic M21 cell extracts (Figure 4B), indicating that the predominant protein-binding element was localized between 219 bp and 768 bp of the VPF/VEGF 3′ UTR.

To further narrow down the 3′ UTR sequence involved in the formation of hypoxia-induced RNA–protein complexes, three subfragments of the 3′ 0.5-kb sequence were obtained by PCR and subcloned into transcription vectors (see MATERIALS AND METHODS). When RNA binding/EMSA was performed with these subfragments of 3′ 0.5 kb using both RNase T1 and RNase A to completely digest RNase T1-resistant sequences, the 3′ HSR but not the 3′ CR-1 (control region 1) or CR-2 (control region 2) formed protein complexes. M21 melanoma cell extracts demonstrated two different mobility shift bands (Figure 5A) binding to the 3′ HSR. In response to hypoxia, the lower band was increased two- to threefold, whereas the upper band was decreased. Antisense RNA transcripts did not show any binding activity, indicating sequence specificity in the sense orientation.

When the RNA binding/EMSA with normoxic M21 cell extracts binding to the 3′ HSR probe was performed in the presence of a 50-fold mass excess of either 3′ HSR RNA in the sense and antisense orientation or the 3′ 0.5-kb RNA, only the sense orientation 3′ HSR and 3′ 0.5-kb RNAs competed for binding. Similar competition experiments performed with 3′ CR-1 and 3′ CR-2 transcripts showed no competition with RNA–protein complexes. Thus, the 3′ HSR sequence, which contains two AU-rich elements (AU 1 and AU 2), is a highly specific element for hypoxia-regulated RNA-binding proteins, suggesting that this region potentially regulates mRNA stability through these RNA-binding proteins.

VPF/VEGF 3′ HSR Element Has a Stem Loop Secondary Structure

Because the 125-bp 3′ HSR sequence showed hypoxia-induced RNA–protein complexes in M21 cells, the importance of secondary structure that might be required for protein recognition was investigated by performing an RNA-folding algorithm, MUFOLD (Jaeger *et al.*, 1989a,b; Zuker, 1989). The resulting secondary folding pattern (Figure 6) incorporates the two AU-rich regions (AU 1 and AU 2) in a stem loop configuration. The folding energy of the stem loop formed by just the AU 1 and AU 2 regions was −28.4 Kcal/mol and −16.5 Kcal/mol for the entire 3′ HSR region. The potential for stem loop protein recognition by RNA-binding proteins has already been established in other systems such as the iron regulatory element-binding proteins (Aziz and Munro, 1987).

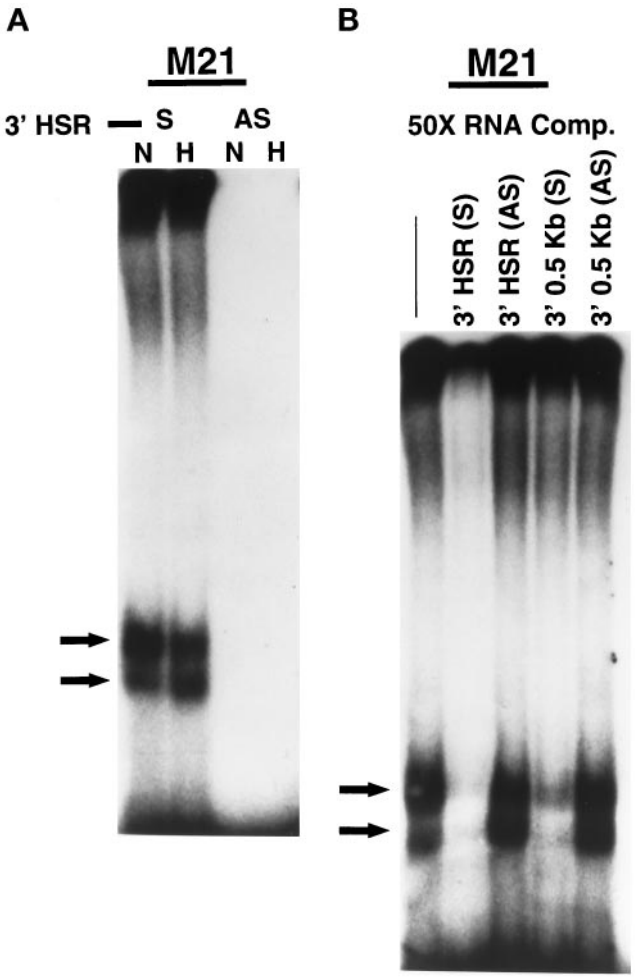

Figure 5. Hypoxia-inducible RNA–protein complexes form with the VPF/VEGF AU-rich 3′ HSR sequence in M21 cells. (A) RNA binding/EMSA was performed with an RNA transcript probe (3′ HSR). RNA–protein complexes were detected in the presence of both RNase T1 and RNase A. Orientation-specific RNA–protein complexes were detected by using sense (S) and antisense (AS) 3′ HSR probes and 24-h normoxic (N) and hypoxic (H) extracts. RNase-resistant complexes are indicated by arrows. Note the hypoxic induction of the faster mobility complex. (B) RNA–protein complexes competed with sense but not antisense RNA containing the 3′ HSR sequence. A 3′ HSR probe was used to perform RNA binding/EMSA with M21 normoxic cell extract without (−) and with a 50-fold excess of sense (S) or antisense (AS) 3′ HSR or 3′ 0.5-kb transcripts.

VPF/VEGF 3′ HSR Confers Increased Expression of a Luciferase–3′ HSR Chimeric mRNA under Hypoxic Conditions

To evaluate whether VPF/VEGF mRNA elements can promote gene expression by increasing mRNA stability, we designed luciferase-VPF/VEGF mRNA chimeric constructs under the control of a constitutive cytomegalovirus enhancer/promoter (see Figure 7A). The constructs have VPF/VEGF cDNA sequences consisting of the whole 3′ UTR, as well as the 3′ HSR and 3′ CR-1 elements, inserted between the luciferase coding sequence and the polyadenylation site. The vectors were transfected into M21 cells and were placed in normoxic or hypoxic conditions for 18 h. The luciferase expression of the control vector showed only a moderate increase in luciferase activity under hypoxia, whereas the luciferase-VPF/VEGF 3′ UTR vector showed appreciable up-regulation (Figure 7B). Luciferase chimeras containing the 3′ HSR element showed a dramatic and statistically significant increase in activity under hypoxic conditions versus normoxia, twofold with $p < 0.04$. The 3′ CR-1 element, which is identical in size to the 3′ HSR element, showed no difference in activity with hypoxia and thus serves as a size-dependent control. As described above, the 3′ HSR element was the only part of the VPF/VEGF mRNA that showed appreciable RNA-binding activity, and thus the hypoxia-induced luciferase data correlate well with in vitro protein binding.

Distinct Proteins Bind to the AU-Rich VPF/VEGF 3′ HSR Regulatory Sequence

After establishing the AU-rich 3′ UTR sequence of human VPF/VEGF mRNA as a potential binding site for mRNA-binding proteins and as a key regulator of mRNA accumulation under hypoxia, we sought to identify specific proteins binding to this region. RNA binding/EMSA experiments were performed with normoxic and hypoxic M21 cell extracts, and the complexes were covalently cross-linked before separation on reducing SDS-polyacrylamide gels. SDS-PAGE analysis of RNA cross-linked proteins using hypoxia-induced M21 cell extracts showed hypoxia–up-regulated bands of at least five distinct species. Most prominent were a doublet at 90/88-kDa, and 72-kDa, 56-kDa, and 46-kDa species (Figure 8A). These hypoxia-induced proteins were consistently represented in at least four independent extracts. The 40-kDa band had only moderate hypoxia induction in additional experiments. In addition, several bands were not extract dependent as indicated by a nonextract control (Figure 8A, lane B).

To examine the specificity of the UV-cross-linked proteins to the VPF/VEGF 3′ HSR, a competition with cold excess 3′HSR RNA was performed. Increasing concentrations of 1- to 50-fold excess demonstrated increased competition for binding to the 90/88-kDa doublet and the 60-kDa bands (Figure 8B). The 72-kDa, 56-kDa, and 46-kDa bands did not compete as well with cold 3′ HSR element, suggesting that they may be less specific RNA-binding proteins for this sequence. Thus, this analysis defined the 90/88-kDa doublet and the 60-kDa species as the most prominent hypoxia-induced VPF/VEGF 3′ HSR-binding proteins. Identification and characterization of the speci-

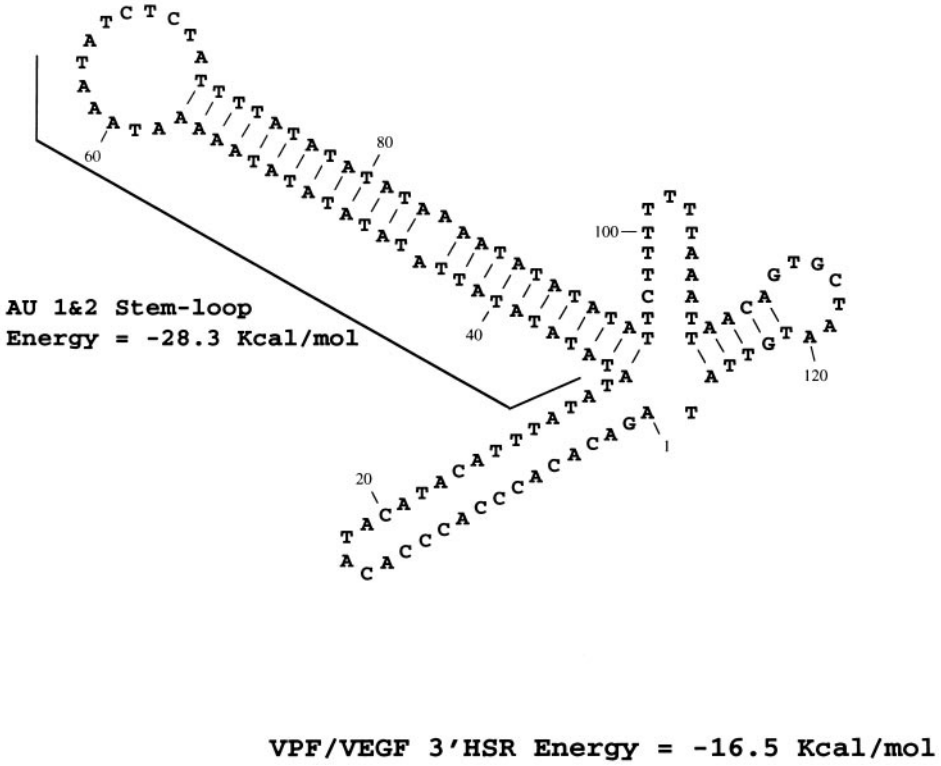

Figure 6. Stem loop secondary structure of the VPF/VEGF AU-rich 3′ HSR. Secondary structure of the 125-bp 3′ HSR sequence within the VPF/VEGF 3′ UTR as determined by MUFOLD (Jaeger *et al.*, 1989a,b; Zuker, 1989). Potential RNA loop structure energies for the AU-rich regions 1 and 2 alone and the whole 3′ HSR are indicated.

ficity of these protein species supports the hypothesis that they play a key role in regulating hypoxia-induced mRNA stability induced by this VPF/VEGF 3′ HSR.

DISCUSSION

There is considerable evidence that increased release of VPF/VEGF may be critical to tumor cell survival under adverse metabolic conditions. In particular, high levels of VPF/VEGF expression have been detected in conditions characterized by tissue hypoxia, such as skin wounds, diabetic retinopathy, and solid tumors. In agreement with previous reports on human cell lines (Claffey and Robinson, 1996), we detected a 6.5-fold increased expression of VPF/VEGF mRNA in the malignant human melanoma line M21 under hypoxic conditions.

To examine the regulatory mechanisms leading to hypoxia-induced VPF/VEGF expression in the M21 melanoma cell line, *VPF/VEGF* gene transcription and mRNA stability were evaluated under normoxic and hypoxic conditions. Transcription was significantly increased by hypoxia by 2.7-fold. This is in accordance with a recent report demonstrating that hypoxia-induced VPF/VEGF transcription was mediated through 5′ flanking gene elements that contain binding sites for the hypoxia-inducible factor 1 transcriptional activator (Wang and Semenza, 1993; Minchenko *et al.*, 1994; Levy *et al.*, 1995; Liu *et al.*, 1995).

VPF/VEGF mRNA stability was found to be a significant factor in hypoxia-induced VPF/VEGF mRNA expression, demonstrating a 1.8-fold increase in M21 cells. Other similar mRNA stability experiments performed on brain-derived human gliobastoma cells revealed up to a fourfold hypoxia-induced mRNA stability (our unpublished results). The extent of VPF/VEGF hypoxia-induced mRNA stability may be distinctly tissue or cell-type dependent. It is likely that skin-derived cells may be less responsive to hypoxia than brain cells and thus their VPF/VEGF stability control is minimized. In an effort to identify mRNA elements that might modulate mRNA stability through RNA–protein interactions, the FL VPF/VEGF mRNA as well as distinct parts were screened by a RNA-binding/EMSA system. We identified an AU-rich 3′ UTR sequence as the major region responsible for RNA-binding activity in M21 cell extracts. The RNA-binding element was found to interact with hypoxia-induced proteins. In addition, a chimeric luciferase reporter gene containing this element was significantly induced under hypoxic conditions, whereas an identical size element that is not recognized by RNA-binding proteins was unaffected. The 125-bp 3′ UTR element, termed 3′ HSR, was found to have a unique stem loop structure consisting of two adjacent

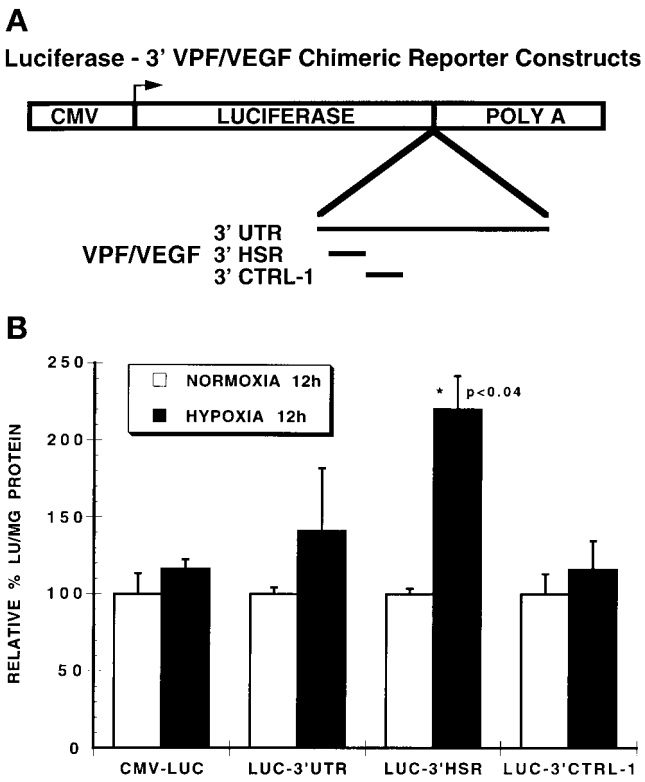

Figure 7. VPF/VEGF 3′ HSR confers increased hypoxia expression to a constitutively expressed luciferase-VPF/VEGF chimeric construct. (A) Schematic model of cytomegalovirus-enhancer/promoter-driven luciferase-VPF/VEGF reporter constructs. VPF/VEGF 3′ UTR elements in the sense orientation were cloned 3′ to luciferase sequence. (B) Luciferase activity of transient transfected M21 cells under normoxic or hypoxic conditions for 12 h (n = 3). Luciferase activity was normalized to normoxic light units/mg of protein to account for differences in transfection efficiency. *p value for *t* test of hypoxic compared with normoxic conditions.

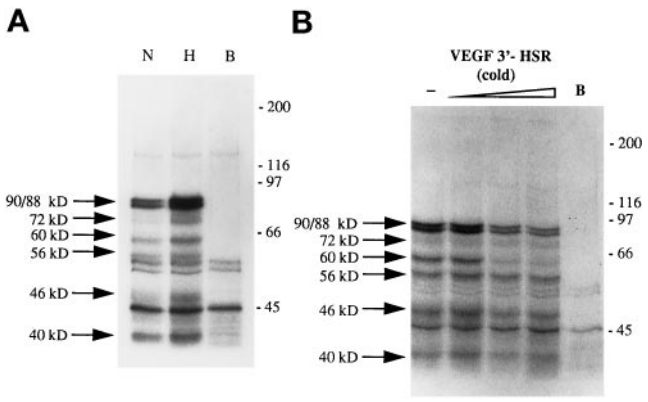

Figure 8. Identification of hypoxia-induced RNA-binding proteins using EMSA/UV-cross-linking and RNA affinity chromatography. (A) Normoxic (N) and hypoxic (H) M21 cell extracts bound to the 3′ HSR probe were subjected to UV-cross-linking/RNase treatment and analyzed by reducing SDS-PAGE. Hypoxia-induced proteins covalently cross-linked to the 3′ HSR probe are indicated by arrows. (B) Competitive inhibition of RNA–protein complex formation by excess cold VPF/VEGF 3′ HSR. M21 24-h hypoxic cell extracts EMSA/UV cross-linked to VPF/VEGF 3′ HSR mRNA (−) was competed with unlabeled VEGF 3′ HSR (0.05, 0.5, and 1 μg 3′ HSR, lanes 2–4, respectively). The arrows indicate 3′ HSR mRNA protein complexes.

AU-rich elements. Further experiments will determine whether this structure is required for hypoxia-induced protein binding.

Five protein species of 90/88 kDa, 72 kDa, 60 kDa, 56 kDa, and 46 kDa, which bind to this AU-rich VPF/VEGF mRNA element, were found to be hypoxia induced. However, only the 90/88 kDa and the 60 kDa were specifically competed with excess cold 3′ HSR RNA. There is one AUUUA sequence within the VPF/VEGF 125-bp 3′ HSR; however, the binding proteins described here do not appear to be the same as the 15–40-kDa species of proteins that have been identified as specific binding proteins for this element, including AU-binding factor 1, AU-A/B and C proteins, AU-binding protein, and AUH factor. Interestingly, Levy *et al*. (1996) have recently identified a hypoxia-inducible 65-kDa protein that binds to the rat VPF/VEGF 3′ UTR sequence, which could approximate the 60-kDa species we observe here. However, the two adjacent AU-rich sequence identified by our analysis in human VPF/VEGF 3′ UTR is not present in the rat 3′ UTR (Levy *et al*., 1996). Purification and complete characterization of these hypoxia-induced VPF/VEGF mRNA-binding proteins will be required to evaluate their interactions with other proteins and mRNAs and their role in regulating VPF/VEGF mRNA stability.

The identification of a distinct, AU-rich HSR in the 3′ UTR of human VPF/VEGF mRNA that is recognized by hypoxia, along with the identification of hypoxia-inducible RNA-binding proteins, is a significant step to further our understanding of the complicated mechanisms that regulate the expression of this potent angiogenic cytokine in response to oxygen stress.

ACKNOWLEDGMENTS

This work was supported in part by National Institutes of Health grants CA-64436 (to K.P.C.), CA-59184 (to M.D.), AG-13314, and CA-66271–04, by the Massachusetts Department of Public Health Breast Cancer Research Program (to S.W.L.), and by the V. Kann Rasmussen Foundation (to K.P.C.). Thanks to Carol Foss for her assistance in the preparation of this article.

REFERENCES

Adamis, A.P., Miller, J.W., Bernal, M.T., D'Amico, D.J., Folkman, J., Yeo, T.K., and Yeo, K.T. (1994). Increased vascular endothelial growth factor levels in the vitreous of eyes with proliferative diabetic retinopathy. Am. J. Ophthalmol. *118*, 445–450.

Aiello, L.P., *et al.* (1994). Vascular endothelial growth factor in ocular fluid of patients with diabetic retinopathy and other retinal disorders [see comments]. N. Engl. J. Med. *331*, 1480–1487.

Alon, T., Hemo, I., Itin, A., Pe'er, J., Stone, J., and Keshet, E. (1995). Vascular endothelial growth factor acts as a survival factor for newly formed retinal vessels and has implications for retinopathy of prematurity. Nat. Med. *1*, 1024–1028.

Aziz, N., and Munro, H.N. (1987). Iron regulates ferritin mRNA translation through a segment of its 5′ untranslated region. Proc. Natl. Acad. Sci. USA *84*, 8478–8482.

Bohjanen, P.R., Petryniak, B., June, C.H., Thompson, C.B., and Lindsten, T. (1991). An inducible cytoplasmic factor (AU-B) binds selectively to AUUUA multimers in the 3′ untranslated region of lymphokine mRNA. Mol. Cell. Biol. *11*, 3288–3295.

Bohjanen, P.R., Petryniak, B., June, C.H., Thompson, C.B., and Lindsten, T. (1992). AU RNA-binding factors differ in their binding specificities and affinities. J. Biol. Chem. *267*, 6302–6309.

Brewer, G. (1991). An A + U-rich element RNA-binding factor regulates c-*myc* mRNA stability in vitro. Mol. Cell. Biol. *11*, 2460–2466.

Brown, L., Berse, B., Jackman, R., Tognazzi, K., Guidi, A., Dvorak, H., Senger, D., Connolly, J., and Schnitt, S. (1995a). Expression of vascular permeability factor (vascular endothelial growth factor) and its receptors in breast cancer. Hum. Pathol. *26*, 86–91.

Brown, L.F., Berse, B., Jackman, R.W., Tognazzi, K., Manseau, E.J., Dvorak, H.F., and Senger, D.R. (1993a). Increased expression of vascular permeability factor (vascular endothelial growth factor) and its receptors in kidney and bladder carcinomas. Am. J. Pathol. *143*, 1255–1262.

Brown, L.F., Berse, B., Jackman, R.W., Tognazzi, K., Manseau, E.J., Senger, D.R., and Dvorak, H.F. (1993b). Expression of vascular permeability factor (vascular endothelial growth factor) and its receptors in adenocarcinomas of the gastrointestinal tract. Cancer Res. *53*, 4727–4735.

Brown, L.F., Olbricht, S.M., Berse, B., Jackman, R.W., Matsueda, G., Tognazzi, K.A., Manseau, E.J., Dvorak, H.F., and Van De Water, L. (1995b). Overexpression of vascular permeability factor (VPF/VEGF) and its endothelial cell receptors in delayed hypersensitivity skin reactions. J. Immunol. *154*, 2801–2807.

Chen, C.Y., and Shyu, A.B. (1995). AU-rich elements: characterization and importance in mRNA degradation. Trends Biochem. Sci. *20*, 465–470.

Claffey, K.P., Brown, L.F., del Aguila, L.F., Tognazzi, K., Yeo, K.T., Manseau, E.J., and Dvorak, H.F. (1996). Expression of vascular permeability factor/vascular endothelial growth factor by melanoma cells increases tumor growth, angiogenesis, and experimental metastasis. Cancer Res. *56*, 172–181.

Claffey, K.P., and Robinson, G.S. (1996). Regulation of VEGF/VPF expression in tumor cells: consequences for tumor growth and metastasis. Cancer Metastasis Rev. *15*, 165–176.

Conn, G., Bayne, M.L., Soderman, D.D., Kwok, P.W., Sullivan, K.A., Palisi, T.M., Hope, D.A., and Thomas, K.A. (1990). Amino acid and cDNA sequences of a vascular endothelial cell mitogen that is homologous to platelet-derived growth factor. Proc. Natl. Acad. Sci. USA *87*, 2628–2632.

Connolly, D.T., Heuvelman, D.M., Nelson, R., Olander, J.V., Eppley, B.L., Delfino, J.J., Siegel, N.R., Leimgruber, R.M., and Feder, J. (1989). Tumor vascular permeability factor stimulates endothelial cell growth and angiogenesis. J. Clin. Invest. *84*, 1470–1478.

Czyzyk-Krzeska, M.F., and Beresh, J.E. (1996). Characterization of the hypoxia-inducible protein binding site within the pyrimidine-rich tract in the 3′-untranslated region of the tyrosine hydroxylase mRNA. J. Biol. Chem. *271*, 3293–3299.

Czyzyk-Krzeska, M.F., Dominski, Z., Kole, R., and Millhorn, D.E. (1994a). Hypoxia stimulates binding of a cytoplasmic protein to a pyrimidine-rich sequence in the 3′-untranslated region of rat tyrosine hydroxylase mRNA. J. Biol. Chem. *269*, 9940–9945.

Czyzyk-Krzeska, M.F., Furnari, B.A., Lawson, E.E., and Millhorn, D.E. (1994b). Hypoxia increases rate of transcription and stability of tyrosine hydroxylase mRNA in pheochromocytoma (PC12) cells. J. Biol. Chem. *269*, 760–764.

Dvorak, H.F., Nagy, J.A., Berse, B., Brown, L.F., Yeo, K.-T., Yeo, T.-K., Dvorak, A.M., Van De Water, L., Sioussat, T.M., and Senger, D.R. (1992). Vascular permeability factor, fibrin, and the pathogenesis of tumor stroma formation. Ann. N.Y. Acad. Sci. *667*, 101–111.

Ebert, B.L., Firth, J.D., and Ratcliffe, P.J. (1995). Hypoxia and mitochondrial inhibitors regulate expression of glucose transporter-1 via distinct *cis*-acting sequences. J. Biol. Chem. *270*, 29083–29089.

Fava, R., Olsen, N., Spencer-Green, G., Yeo, K.-T., Yeo, T.-K., Berse, B., Jackman, R., Senger, D., Dvorak, H., and Brown, L. (1994). Vascular permeability factor/endothelial growth factor (VPF/VEGF): accumulation and expression in human synovial fluids and rheumatoid synovial tissue. J. Exp. Med. *180*, 341–346.

Ferrara, N., and Henzel, W.J. (1989). Pituitary follicular cells secrete a novel heparin-binding growth factor specific for vascular endothelial cells. Biochem. Biophys. Res. Commun. *161*, 851–858.

Ferrara, N., Houck, K.A., Jakeman, L.B., Winer, J., and Leung, D.W. (1991a). The vascular endothelial growth factor family of polypeptides. J. Cell. Biochem. *47*, 211–218.

Ferrara, N., Leung, D.W., Cachianes, G., Winer, J., and Henzel, W.J. (1991b). Purification and cloning of vascular endothelial growth factor secreted by pituitary folliculostellate cells. Methods Enzymol. *198*, 391–405.

Gillis, P., and Malter, J.S. (1991). The adenosine-uridine binding factor recognizes the AU-rich elements of cytokine, lymphokine, and oncogene mRNAs. J. Biol. Chem. *266*, 3172–3177.

Gorospe, M., and Baglioni, C. (1994). Degradation of unstable interleukin-1 alpha mRNA in a rabbit reticulocyte cell-free system. Localization of an instability determinant to a cluster of AUUUA motifs. J. Biol. Chem. *269*, 11845–11851.

Gospodarowicz, D., Abraham, J.A., and Schilling, J. (1989). Isolation and characterization of a vascular endothelial cell mitogen produced by pituitary-derived folliculo stellate cells. Proc. Natl. Acad. Sci. USA *86*, 7311–7315.

Graven, K.K., Troxler, R.F., Kornfeld, H., Panchenko, M.V., and Farber, H.W. (1994). Regulation of endothelial cell glyceraldehyde-3-phosphate dehydrogenase expression by hypoxia. J. Biol. Chem. *269*, 24446–24453.

Hashimoto, E., Ogita, T., Nakaoka, T., Matsuoka, R., Takao, A., and Kira, Y. (1994). Rapid induction of vascular endothelial growth factor expression by transient ischemia in rat heart. Am. J. Physiol. *267*, 1948–1954.

Ikeda, E., Achen, M.G., Breier, G., and Risau, W. (1995). Hypoxia-induced transcriptional activation and increased mRNA stability of vascular endothelial growth factor in C6 glioma cells. J. Biol. Chem. *270*, 19761–19766.

Jaeger, J.A., Turner, D.H., and Zuker, M. (1989a). Improved predictions of secondary structures for RNA. Proc. Natl. Acad. Sci. USA *86*, 7706–7710.

Jaeger, J.A., Turner, D.H., and Zuker, M. (1989b). Predicting optimal and suboptimal secondary structure for RNA. Methods Enzymol. *183*, 281–306.

Katz, D.A., Theodorakis, N.G., Cleveland, D.W., Lindsten, T., and Thompson, C.B. (1994). AU-A, an RNA-binding activity distinct from hnRNP A1, is selective for AUUUA repeats and shuttles between the nucleus and the cytoplasm. Nucleic Acids Res. *22*, 238–246.

Keck, P.J., Hauser, S.D., Krivi, G., Sanzo, K., Warren, T., Feder, J., and Connolly, D.T. (1989). Vascular permeability factor, an endothelial cell mitogen related to PDGF. Science *246*, 1309–1312.

Ladoux, A., and Frelin, C. (1993). Hypoxia is a strong inducer of vascular endothelial growth factor mRNA expression in the heart. Biochem. Biophys. Res. Commun. *195*, 1005–1010.

Lagnado, C.A., Brown, C.Y., and Goodall, G.J. (1994). AUUUA is not sufficient to promote poly(A) shortening and degradation of an mRNA: the functional sequence within AU-rich elements may be UUAUUUA(U/A)(U/A). Mol. Cell. Biol. *14*, 7984–7995.

Lee, S.W., Tomasetto, C., and Sager, R. (1991). Positive selection of candidate tumor-suppressor genes by subtractive hybridization. Proc. Natl. Acad. Sci. USA *88*, 2825–2829.

Leung, D.W., Cachianes, G., Kuang, W.J., Goeddel, D.V., and Ferrara, N. (1989). Vascular endothelial growth factor is a secreted angiogenic mitogen. Science *246*, 1306–1309.

Levy, A.P., Levy, N.S., and Goldberg, M.A. (1996a). Hypoxia-inducible protein binding to vascular endothelial growth factor mRNA and its modulation by the von Hippel-Lindau protein. J. Biol. Chem. *271*, 25492–25497.

Levy, A.P., Levy, N.S., and Goldberg, M.A. (1996b). Post-transcriptional regulation of vascular endothelial growth factor by hypoxia. J. Biol. Chem. *271*, 2746–2753.

Levy, A.P., Levy, N.S., Wegner, S., and Goldberg, M.A. (1995). Transcriptional regulation of the rat vascular endothelial growth factor gene by hypoxia. J. Biol. Chem. *270*, 13333–13340.

Levy, A.P., Tamargo, R., Brem, H., and Nathans, D. (1989). An endothelial cell growth factor from the mouse neuroblastoma cell line NB41. Growth Factors *2*, 9–19.

Liu, Y., Cox, S.R., Morita, T., and Kourembanas, S. (1995). Hypoxia regulates vascular endothelial growth factor gene expression in endothelial cells. Identification of a 5′ enhancer. Circ. Res. *77*, 638–643.

Malter, J.S. (1989). Identification of an AUUUA-specific messenger RNA binding protein. Science *246*, 664–666.

Malter, J.S., and Hong, Y. (1991). A redox switch and phosphorylation are involved in the post-translational up-regulation of the adenosine-uridine binding factor by phorbol ester and ionophore. J. Biol. Chem. *266*, 3167–3171.

Masiakowski, P., Breathnach, R., Bloch, J., Gannon, F., Krust, A., and Chambon, P. (1983). Cloning of cDNA sequences of hormone-regulated genes from the MCF-7 human breast cancer cell line. Nucleic Acids Res. *10*, 7895–7903.

Minchenko, A., Salceda, S., Bauer, T., and Caro, J. (1994). Hypoxia regulatory elements of the human vascular endothelial growth factor gene. Cell. Mol. Biol. *40*, 35–39.

Mukhopadhyay, D., Tsiokas, L., Zhou, X.M., Foster, D., Brugge, J.S., and Sukhatme, V.P. (1995). Hypoxic induction of human vascular endothelial growth factor expression through c-*Src* activation. Nature *375*, 577–581.

Nagy, E., and Rigby, W.F. (1995). Glyceraldehyde-3-phosphate dehydrogenase selectively binds AU-rich RNA in the NAD(+)-binding region (Rossmann fold). J. Biol. Chem. *270*, 2755–2763.

Nakagawa, J., Waldner, H., Meyer-Monard, S., Hofsteenge, J., Jeno, P., and Moroni, C. (1995). AUH, a gene encoding an AU-specific RNA binding protein with intrinsic enoyl-CoA hydratase activity. Proc. Natl. Acad. Sci. USA *92*, 2051–2055.

Pierce, E.A., Avery, R.L., Foley, E.D., Aiello, L.P., and Smith, L.E. (1995). Vascular endothelial growth factor/vascular permeability factor expression in a mouse model of retinal neovascularization. Proc. Natl. Acad. Sci. USA *92*, 905–909.

Plate, K.H., Breier, G., Weich, H.A., and Risau, W. (1992). Vascular endothelial growth factor is a potential tumour angiogenesis factor in human gliomas in vivo. Nature *359*, 845–848.

Sabri, M.N., DiSciascio, G., Cowley, M.J., Alpert, D., and Vetrovec, G.W. (1991). Coronary collateral recruitment: functional significance and relation to rate of vessel closure. Am. Heart J. *121*, 876–880.

Schuler, G.D., and Cole, M.D. (1988). GM-CSF and oncogene mRNA stabilities are independently regulated in trans in a mouse monocytic tumor. Cell *55*, 1115–1122.

Senger, D.R., Connolly, D.T., Van De Water, L., Feder, J., and Dvorak, H.F. (1990). Purification and NH_2-terminal amino acid sequence of guinea pig tumor-secreted vascular permeability factor. Cancer Res. *50*, 1774–1778.

Shaw, G., and Kamen, R. (1986). A conserved AU sequence from the 3′ untranslated region of GM-CSF mRNA mediates selective mRNA degradation. Cell *46*, 659–667.

Shima, D.T., Deutsch, U., and D'Amore, P.A. (1995). Hypoxic induction of vascular endothelial growth factor (VEGF) in human epithelial cells is mediated by increases in mRNA stability. FEBS Lett. *370*, 203–208.

Shweiki, D., Itin, A., Soffer, D., and Keshet, E. (1992). Vascular endothelial growth factor induced by hypoxia may mediate hypoxia-initiated angiogenesis. Nature *359*, 843–845.

Stein, I., Neeman, M., Shweiki, D., Itin, A., and Keshet, E. (1995). Stabilization of vascular endothelial growth factor mRNA by hypoxia and hypoglycemia and coregulation with other ischemia-induced genes. Mol. Cell. Biol. *15*, 5363–5368.

Stephens, C.M., and Bauerle, R. (1992). Essential cysteines in 3-deoxy-D-arabino-heptulosonate-7-phosphate synthase from *Escherichia coli*. Analysis by chemical modification and site-directed mutagenesis of the phenylalanine-sensitive isozyme. J. Biol. Chem. *267*, 5762–5767.

Stone, J., Itin, A., Alon, T., Pe'er, J., Gnessin, H., Chan-Ling, T., and Keshet, E. (1995). Development of retinal vasculature is mediated by hypoxia-induced vascular endothelial growth factor (VEGF) expression by neuroglia. J. Neurosci. *15*, 4738–4747.

Tischer, E., Mitchell, R., Hartman, T., Silva, M., Gospodarowicz, D., Fiddes, J.C., and Abraham, J.A. (1991). The human gene for vascular endothelial growth factor. Multiple protein forms are encoded through alternative exon splicing. J. Biol. Chem. *266*, 11947–11954.

Vakalopoulou, E., Schaack, J., and Shenk, T. (1991). A 32-kilodalton protein binds to AU-rich domains in the 3′ untranslated regions of rapidly degraded mRNAs. Mol. Cell. Biol. *11*, 3355–3364.

Wang, G.L., and Semenza, G.L. (1993). Characterization of hypoxia-inducible factor 1 and regulation of DNA binding activity by hypoxia. J. Biol. Chem. *268*, 21513–21518.

Wang, X., Kiledjian, M., Weiss, I.M., and Liebhaber, S.A. (1995). Detection and characterization of a 3′ untranslated region ribonucleoprotein complex associated with human alpha-globin mRNA stability (published erratum appears in Mol. Cell. Biol. *15*:2331, 1995). Mol. Cell. Biol. *15*, 1769–1777.

Weindel, K., Moringlane, J.R., Marme, D., and Weich, H.A. (1994). Detection and quantification of vascular endothelial growth factor/vascular permeability factor in brain tumor tissue and cyst fluid: the key to angiogenesis? Neurosurgery *35*, 439–448; discussion 448–439.

You, Y., Chen, C.Y., and Shyu, A.B. (1992). U-rich sequence-binding proteins (URBPs) interacting with a 20-nucleotide U-rich sequence

in the 3′ untranslated region of c-*fos* mRNA may be involved in the first step of c-*fos* mRNA degradation. Mol. Cell. Biol. *12*, 2931–2940.

Zhang, W., Wagner, B.J., Ehrenman, K., Schaefer, A.W., DeMaria, C.T., Crater, D., DeHaven, K., Long, L., and Brewer, G. (1993). Purification, characterization, and cDNA cloning of an AU-rich element RNA-binding protein, AUF1. Mol. Cell. Biol. *13*, 7652–7665.

Zubiaga, A.M., Belasco, J.G., and Greenberg, M.E. (1995). The nonamer UUAUUUAUU is the key AU-rich sequence motif that mediates mRNA degradation. Mol. Cell. Biol. *15*, 2219–2230.

Zuker, M. (1989). On finding all suboptimal foldings of an RNA molecule. Science *244*, 48–52.